Characteristics of rising tone whistler mode waves inside the Earth's plasmasphere, plasmaspheric plumes and plasmatrough

S. Teng[1,2,3], W. Li[3], X. Tao[1,2], X.-C. Shen[3], and Q. Ma[4,3]

[1]CAS Key Laboratory of Geospace Environment, Department of Geophysics and Planetary Sciences, University of Science and Technology of China, Hefei, China

[2]CAS Center for Excellence in Comparative Planetology, China

[3]Center for Space Physics, Boston University, Boston, Massachusetts, USA

[4]Department of Atmospheric and Oceanic Sciences, University of California, Los Angeles, Los Angeles, California, USA

Corresponding author: W. Li (luckymoon761@gmail.com)

Key Points:

- Rising tone whistler mode waves are statistically analyzed inside the plasmasphere, plasmaspheric plumes and plasmatrough.
- Among these three regions, the occurrence rate of rising tone whistler mode waves in plasmapheric plumes is the highest.
- Inside the plasmasphere and plumes, rising tone whistler mode waves tend to be more field-aligned than those outside the plasmapause.

Abstract

Whistler mode waves, particularly rising tone emissions, are important for nonlinear interactions with energetic electrons in the Earth's magnetosphere. In this letter, we evaluate the characteristics of rising tone whistler mode waves in three distinct regions: 1. inside the plasmasphere; 2. plasmapheric plumes, and 3. plasmatrough (outside the plasmapause). Our statistical results indicate that the occurrence rate of rising tone emissions tends to increase with increasing geomagnetic activity and is highest in plasmaspheric plumes among these three regions. Inside the plasmasphere, rising tone emissions typically occur in the outer portion of the plasmasphere, particularly near the dawnside. Moreover, the rising tone emissions inside the plasmasphere and plumes tend to be more field aligned than those in the plasmatrough. Our new findings of global wave properties of rising tone emissions are critical for understanding the generation of rising tone emissions and their effects on radiation belt electron dynamics.

Plain Language Summary

Rising tone whistler mode waves are intense electromagnetic emissions and commonly present in the Earth's magnetosphere. They are typically observed in the plasmatrough, which is a low-density region outside the plasmapause. By analyzing the high time resolution magnetic wave data from Van Allen Probes measurements, we present the global distribution and characteristics of rising tone whistler mode waves in three different regions: inside the plasmasphere, plasmaspheric plumes and the plasmatrough. Among these three regions, the occurrence rate of rising tone emissions is found to be highest in plasmaspheric plumes. The rising tone emissions observed inside the plasmasphere and plumes tend to be more field-aligned than those in the plasmatrough. Our new findings of global wave properties of rising tone emissions are critical for understanding the generation of rising tone emissions and their effects on radiation belt electron dynamics.

1 Introduction

Whistler mode chorus waves are intense coherent electromagnetic emissions exhibiting discrete rising or falling tones, and typically occur in two distinct frequency bands: a lower band and an upper band with a power minimum at 0.5 f_{ce} (Burtis and Helliwell, 1975; Santolík et al., 2004; Tsurutani and Smith, 1974), where f_{ce} is the equatorial electron cyclotron frequency. These waves play a crucial role in radiation belt electron dynamics, through effectively accelerating 100s keV electrons to MeV energies in the outer radiation belt (Horne et al., 2005; Reeves et al., 2013; Thorne et al., 2013) and causing precipitation of electrons to form diffuse and pulsating aurora in the Earth's upper atmosphere (Ni et al., 2008, 2016; Nishimura et al., 2010; Thorne et al., 2010).

The generation region of chorus is known to be mostly located in the low-density region outside the plasmapause, which is also called plasmatrough, near the geomagnetic equator (LeDocq et al., 1998; Santolík et al., 2003). Previous statistical studies have shown that whistler mode chorus waves have a high occurrence rate from the midnight to the noon sector (Li et al., 2009, 2011a; Meredith et al., 2003, 2012). In contrast, plasmaspheric hiss is typically observed in the high-density region inside the plasmasphere or plasmaspheric plumes, preferentially from the dawn to the dusk sector (Meredith et al., 2004, 2018; Li et al., 2015; Shi et al., 2019; Summers et al., 2008; Thorne et al., 1973). Plasmaspheric hiss and chorus waves overlap in frequency (Tsurutani and Smith, 1977). However, chorus waves are typically narrowband and quasi-coherent (Albert et al., 2012; Artemyev et al., 2012; Bell, 1984; Bortnik et al., 2008a; Inan et al., 1978; Kellogg et al., 2010; Omura et al., 2007; Tao and Bortnik, 2010; Tao et al., 2012), while plasmaspheric hiss is normally incoherent and unstructured (Bortnik et al., 2008b; Thorne et al., 1973). The generation mechanisms of chorus and hiss are still under active investigation. Although it is widely accepted that the generation of chorus waves is nonlinear (Helliwell, 1967; Nunn, 1971; Omura et al., 2008; Soto-Chavez et al., 2014; Tao et al., 2017a,b; Trakhtengerts, 1995; Vomvoridis et al., 1982), the detailed process is still an on-going topic. Potential generation mechanisms of plasmaspheric hiss include local excitation by electron cyclotron instability (Solomon et al., 1988; Tsurutani et al., 2015), propagation effects of chorus waves into the plasmasphere (Agapitov et al., 2018; Bortnik et al., 2008b; Chen et al., 2012; Meredith et al., 2013), and origination from lightning generated whistlers (Green et al., 2005).

Plasmaspheric plumes have attracted increasing attention in recent years because of their favorable conditions for generating various types of plasma waves. Some case studies reported that plasmaspheric hiss is likely locally excited in plasmaspheric plumes (Laakso et al., 2015; Su et al., 2018). Shi et al. (2019) proposed that the majority of whistler mode waves in plumes are locally amplified in association with energetic electron injection. Hartley et al. (2019) suggested that only an extremely small fraction of chorus waves can propagate into the plasmasphere except for chorus waves near the edge of plasmaspheric plumes. These plume whistler mode waves are found to be potentially very effective in energetic electron precipitation loss (e.g., Li et al., 2019; Summers et al., 2008; Zhang et al., 2018). Case studies also show that whistler mode waves in plumes exhibit either rising tones (Shi et al., 2019; Su et al., 2018) or hiss-like emissions (Li et al., 2019). However, the occurrence of rising tone emissions in plasmaspheric plumes has not been systematically studied yet. Although the characteristics of whistler mode waves including rising and falling tones outside the plasmasphere are studied extensively (e.g., Gao et al., 2014; Li et al., 2011b, 2012; Santolik et al., 2003, 2009), there is still a lack of understanding about the global distribution of rising tone whistler mode waves inside the plasmasphere and plasmaspheric plumes.

In this letter, we aim to evaluate the global distribution and characteristics of rising tone whistler mode waves in three distinct regions: (1) inside the plasmasphere, (2) in the plasmaspheric plumes, and (3) in the plasmatrough (outside the plasmapause). Moreover, we investigate the wave normal angle distributions of rising tone whistler mode emissions in these three regions to provide insights into understanding wave generation and propagation.

2 Data analysis

In this study, we utilize Van Allen Probes data from October 2012 to May 2016 during which both spacecraft completed two full orbital precessions (Kessel et al., 2013; Mauk et al., 2013) and covered all magnetic local times (MLTs) twice. High time resolution measurements from burst mode of Electric and Magnetic Field Instrument Suite and Integrated Science (EMFISIS) (Kletzing et al., 2013) instrument are used to investigate rising tone whistler mode waves. A total of about 1412108 6-second burst-mode waveform data throughout the chosen period were recorded. We set the threshold of minimum magnetic power spectral density to be 10^{-8}nT^2/Hz in the frequency range from 0.1 f_{ce} to 0.8 f_{ce} to eliminate wave spectra without any or very weak signals and then select the bursts containing rising tone discrete elements by visually inspecting the power spectrogram. In this work, each selected 6-second waveform burst mode data is defined as an "event". For the recorded rising tone emissions, we subsequently categorize them into three different groups: (1) inside the plasmasphere, (2) plasmapheric plumes, and (3) plasmatrough. The determination of each region is mainly based on the density profile, which is inferred from the High-Frequency Receiver (HFR) (Kurth et al., 2015) and from the Electric Field and Waves (EFW) instrument (Wygant et al., 2013), as described below.

Following the technique of Moldwin et al. (2002), the plasmapause location is defined as the innermost steep gradient in the electron density profile when the density drops by at least a factor of 5 within a half L shell in any leg (inbound or outbound) of one orbit. If the density keeps constantly high (e.g., larger than 100 cm^{-3}) throughout the leg or no plasmapause crossing is observed, the whole leg is assumed to be inside the plasmasphere. A plume is defined in a region outside the plasmapause. We adopted the criterion of Shi et al. (2019) to choose two referred density values at any observed L shell, which are $N > 1.2 \times \min(N_{lower\ L})$ and $N > 2.5 \times \min(N_{lower\ L}) \times L_n^6 / L^6$. Here $\min(N_{lower\ L})$ is the minimum density between the plasmapause crossing and the satellite location and L_n is the L shell where the minimum density ($N_{lower\ L}$) is recorded. The calculation of L shell and other parameters, such as magnetic latitude (MLat) and MLT, is based on the TS04D model (Tsyganenko and Sitnov, 2005). After applying the method described above, we visually inspected the identified plasmapause location and plume regions to ensure that the automatic identifications are reasonable. We have found 6988 events inside the plasmasphere, 2896 in the plumes and 83879 in the plasmatrough. The majority of rising tone whistler mode emissions are observed outside the plasmapause, but there are still a number of them observed inside the plasmasphere and plasmaspheric plumes.

Figure 1 illustrates three typical examples of rising tone whistler mode waves observed inside the (A) plasmasphere, (B) plasmaspheric plume, and (C) plasmatrough. Since AL index is closely related to substorm activities (e.g., Gjerloev et al., 2004), we show AL (black) and AL* (red) in Figures 1 A-a, B-a and C-a, where AL* is the minimum of AL in the preceding three hours. In Figures 1A-a and B-a, AL* ranged between −300 and −500 nT, indicating a moderate substorm activity. For the case in the plasmatrough in Figure 1C-a, AL* dropped below −500 nT, indicating a strong substorm activity. In Case A, the density (Figure 1b) kept high throughout the whole orbit and no abrupt density gradient was found, and thus this orbit was identified to be located inside the plasmasphere. For Cases B and C, the plasmapause crossings were identified, as marked by blue vertical lines. The plume regions are highlighted by the magenta line in Figure 1B-b. Figures 1c-e show the overview of the WFR electric and magnetic spectrogram and wave normal angle (WNA) in the frequency range of 10 − 10000 Hz. Wave spectrogram and wave normal angles indicate that there exist field-aligned whistler mode waves and oblique magnetosonic waves in three cases. In this study, we mainly focus on rising tone whistler mode emissions, which can only be identified from the burst mode data. Three vertical dashed red lines denote the time of three selected burst intervals. The magnetic wave spectra and wave normal angle of these continuous waveforms over 6 seconds are shown on the bottom for the three occasions. Interestingly, the duration of rising tones in the high-density regions (Cases A and B) is longer than that in a low-density region (Case C), which is consistent with the event reported by Shi et al. (2019). Typical rising tone chorus with short duration (<0.5 s) and a large sweep rate, shown in Figure 1C-f, is not observed inside the plasmasphere and plasmaspheric plumes. While a quantitative analysis of the duration of every rising tone element is beyond the scope of this study, through visually inspecting a large number of wave emissions, we found that this is likely one of the major differences for rising tone emissions in the different regions. Wave normal angles for the three cases (Figure 1g) indicate that rising tone whistler mode waves are quasi-parallel. A statistical WNA analysis of all rising tone events is presented in section 3.

3 Statistical Results of Rising Tone Whistler Mode Emissions in the Three Regions

Figure 2 shows the global distribution of occurrence rate and number of samples of rising tone whistler mode waves observed in the three regions as a function of L shell and MLT, as well as their dependence on AL*. The distributions are categorized by regions inside the plasmasphere (top), plasmaspheric plumes (middle) and plasmatrough (bottom) during quiet (AL* > −100 nT), moderate (−300 < AL* < −100 nT), and active (AL* < −300 nT) geomagnetic conditions. The distributions of occurrence rate, which is the ratio between the number of events and the total number of burst-mode samples in each bin are shown in large panels, with the corresponding number of burst-mode samples shown in small panels. Only the bins with the number of samples larger than 20 are chosen to show the value of occurrence rate to eliminate the statistically insignificant values.

The occurrence rate distribution exhibits a clear dependence on geomagnetic activity for each of three regions. As geomagnetic activities enhance, the occurrence rate increases, which is consistent with previous studies (e.g., Li et al., 2009; Meredith et al., 2012). The number of samples recorded in the plasmaspheric plumes is much smaller than that inside the plasmasphere or plasmatrough, thus the occurrence rate in the plasmaspheric plumes might be statistically less significant than that in the other two regions. Nevertheless, it is very interesting to note that under the same geomagnetic condition, the peak occurrence rate of rising tone emissions in plasmaspheric plumes is the highest (as long as the plumes are detected), followed by the emissions in the plasmatrough. The coexistence of high density cold plasma and energetic particles may provide favorable conditions for rising tone whistler mode wave amplification, which probably accounts for the high occurrence rate. It is worth noting that the high occurrence rates in plasmaspheric plumes are mostly observed at large L shells ($\sim 5-6$). Only during active geomagnetic times when the plasmapause location moves Earthward, rising tone emissions tend to be observed at $L < 5$ near the dusk sector where the plumes are known to preferentially form (e.g., Goldstein et al., 2004; Shi et al., 2019).

Inside the plasmasphere, while the occurrence rate of rising tone emissions is relatively low, there still exist bins with the peak value of occurrence rate up to ~50% near the dawnside at $L > 4.5$ (likely outer portion of the plasmasphere) during active conditions. This may be related to the energetic electron drift into the outer portion of the plasmasphere near the dawn-to-noon sector after their initial injection near the nightside during active conditions (e.g., Li et al., 2013). Note that the shape of plasmapshere is often asymmetric with a compression on the nightside and an extension at large L shells on the dayside as a result of enhanced convection during active times (e.g., Li et al., 2013). Correspondingly, the number of samples inside the plasmasphere is smaller over the night-to-dawn sectors than that over the dawn-to-dusk sector during modest and active conditions.

To compare with the occurrence rate in the above two high-density regions, the bottom panels in Figure 2 show the distribution of rising tone chorus observed in the plasmatrough. Rising tones preferentially occur from the midnight to the afternoon sector, especially during active times, consistent with previous statistical studies (e.g., Li et al., 2009; Meredith et al., 2003, 2012). As expected, the occurrence rate of rising tone chorus increases with increasing geomagnetic activity up to tens of % from the night to the afternoon sector.

Figure 3 presents the normalized probability distribution function (PDF) of f_{pe}/f_{ce} and density in the three different regions, where f_{pe}/f_{ce} is the ratio of plasma frequency to local electron gyrofrequency. Interestingly, there is no clear difference in the density and f_{pe}/f_{ce} distribution between rising tone emissions inside the plasmasphere and plasmaspheric plumes, probably because rising tone emissions detected inside the plasmasphere are distributed in the outer portion of the plasmasphere (at relatively large *L* shells). However, the difference between inside the plasmasphere and outside the plasmapause is very clear. The f_{pe}/f_{ce} distribution in the plasmatrough is much narrower than that inside the plasmasphere or in plumes, and has a pronounced peak at about 4−5, which is consistent with Meredith et al. (2003). On the other hand, in the high-density regions, both inside the plasmasphere and plasmaspheric plumes, the f_{pe}/f_{ce} distribution is much broader and peaks around 11. Since the density and f_{pe}/f_{ce} are closely related, the PDF values of density for the three groups show a similar trend as that of f_{pe}/f_{ce}. Inside the plasmasphere and plasmaspheric plumes, the density distribution is much broader and peaks at a higher value $\sim 40\ cm^{-3}$. However, outside the plasmasphere, the density distribution is very narrow, peaking at $\sim 5\ cm^{-3}$. Previous studies demonstrated that rising tone emissions are preferentially observed in the region with low values of f_{pe}/f_{ce} (Meredith et al., 2003; Li et al., 2012), where the local electron acceleration is the most efficient (Horne et al., 2003). Interestingly, our study indicates that rising tone emissions also exist in the region with high values of f_{pe}/f_{ce}, both inside the plasmasphere and plumes.

Wave normal angle distributions of chorus waves have been extensively studied over the past few decades. Rising tone chorus is shown to be mostly field-aligned (Burton and Holzer, 1974; Cornilleau-Wehrlin et al., 1976; Li et al., 2011b; Taubenschuss et al., 2014), while falling tone chorus typically has a wave normal angle close to the resonance cone (Artemyev et al., 2016; Burton and Holzer, 1974; Cornilleau-Wehrlin et al., 1976; Li et al., 2011b). In this study, we exclude the falling tones and focus on the wave normal angle distribution of rising tone whistler mode waves alone in both upper and lower bands in the three different regions.

To evaluate the detailed wave normal angle distribution, we present the rising tone statistics as a function of wave normal angle and normalized wave frequency in Figure 4. The top panels show the PDF of wave occurrence in three regions. The PDF value of upper and lower band observed in the plasmatrough is close, while the PDF values of upper band observed inside the plasmasphere and plumes are very low. A possible reason could be that the excitation mechanism of upper band chorus waves depends on plasma density or f_{pe}/f_{ce}. The wave normal angle distribution shows that rising tone whistler mode waves both inside the plasmasphere and plasmaspheric plumes tend to peak at about 10°. However, in the plasmatrough, the WNA distribution peaks at $< 20^{\circ}$ for the wave frequency less than $0.3\ f_{ce}$, and tends to peak at larger wave normal angles for the wave frequency higher than $0.3\ f_{ce}$. In all three regions, the wave normal angles of upper band tend to have smaller values at higher frequency, and exhibit a broader distribution just above $0.5\ f_{ce}$. Li et al. (2016) showed that lower band chorus has a quasi-parallel mode and a quasi-electrostatic mode, and the upper band chorus wave normal angle varies between 0° and the resonance cone (Taubenschuss et al., 2014, 2015). The second peak near the resonance cone angle is not very evident in Figure 4 possibly because of the exclusion of falling tone chorus waves, which are typically very oblique, close to the resonance cone (Li et al., 2011b). The middle and bottom panels in Figure 4 show the mean value of magnetic and electric power spectral density in each wave frequency and normal angle bin. The magnetic/electric wave power of upper band in the plasmasphere and plumes are much lower than that of lower band. The magnetic wave power is stronger in plasmaspheric plumes than that inside the plasmasphere, consistent with the findings by Shi et al. (2019). The bottom panels in Figure 4 show that rising tone emissions observed inside the plasmasphere and plasmaspheric plumes have weaker electric wave power compared to chorus waves in the plasmatrough.

4 Summary and Discussion

In this letter, we performed a statistical analysis to evaluate the characteristics of rising tone whistler mode emissions in three different regions: inside the plasmasphere, plasmaspheric plumes, and plasmatrough (outside the plasmapause) using Van Allen Probes waveform data. The main findings are summarized below:

1. Rising tone whistler mode emissions are observed not only in the plasmatrough, but also inside the plasmasphere and plasmaspheric plumes. The occurrence rate of rising tone emissions tends to increase as geomagnetic activity increases. Interestingly, among these three regions, the occurrence rate is highest in plasmaspheric plumes (once the plumes are observed), particularly from the dawn to the dusk sector during active geomagnetic conditions. Inside the plasmasphere, the occurrence rate follows a similar pattern as that in the plasmatrough, but with smaller values. Moreover, the occurrence rate is higher in the outer portion of the plasmasphere, not deep inside the plasmasphere, and is higher from the post-midnight sector to the dawn sector, which is consistent with the electron drift trajectory after injection.

2. The probability distribution of total electron density and f_{pe}/f_{ce} indicates that in the high-density region, both inside the plasmasphere and plumes, the peak values of density (f_{pe}/f_{ce}) are similar, around 40 cm^{-3} (10). However, in the plasmatrough, the peak value of density (f_{pe}/f_{ce}) is much lower, dropping to 10 cm^{-3} (5).

3. The wave normal angle distributions of rising tone whistler mode emissions both inside the plasmasphere and in plumes exhibit only one peak, near the field-aligned direction, whereas rising tone chorus in the plasmatrough tend to have more oblique wave normal angles, particularly at the frequency above 0.3 f_{ce}. The magnetic wave power of rising tone whistler mode emissions in plumes is stronger than that inside the plasmasphere. The electric wave power outside the plasmapause is evidently stronger than that inside the plasmasphere and plumes, especially at higher wave normal angles. Different from rising tone chorus emissions observed in the plasmatrough, very limited upper band rising tone emissions are observed inside the plasmasphere and plumes.

It is important to note that the effects of rising tone emissions, observed in the plasmatrough and plasmasphere/plumes, on energetic electrons are very different, since they occur in the regions with distinct values of f_{pe}/f_{ce}, which is a key factor determining the resonant electron energy. Moreover, the rising tone elements inside the plasmasphere and plasmaspheric plumes appear to last longer than typical chorus waves observed outside the plasmapause, as an example shown in Figure 1, as well as in many other events (not shown). This interesting feature suggests that the duration of rising tone emissions is likely to be closely related to the plasma density or f_{pe}/f_{ce}. The quantitative evaluation of the duration of each rising tone emission is beyond the scope of this present study, and is left for future investigations. Nevertheless, our systematic analysis of rising tone whistler mode waves in three distinct regions provides important information on the wave distribution and characteristics and thus is critical for understanding the generation mechanism of rising tone whistler mode waves and their potential roles in energetic electron dynamics in the Earth's magnetosphere.

Acknowledgments

This work was supported by NSFC grants 41674174 and 41631071. WL, XS, and QM would like to acknowledge the NSF grant AGS-1847818 and the Alfred P. Sloan Research Fellowship FG-2018-10936. We would like to thank the Van Allen Probes team, especially the EMFISIS team for making their data available to the public and the CDAWeb for the use of AL data. Van Allen Probes data from EMFISIS were obtained from the website https://emfisis.physics.uiowa.edu/data/index/, and from EFW were obtained from http://rbsp.space.umn.edu/data/rbsp/.

References

Agapitov, O., Mourenas, D., Artemyev, A., Mozer, F. S., Bonnell, J. W., Angelopoulos, V., Shastun, V., & Krasnoselskikh, V. (2018). Spatial extent and temporal correlation of chorus and hiss: Statistical results from multipoint THEMIS observations. Journal of Geophysical Research: Space Physics, 123, 8317–8330. https://doi.org/10.1029/2018JA025725

Albert, J. M., X. Tao, and J. Bortnik (2012), Aspects of nonlinear wave particle interactions, in Dynamics of the Earth's Radiation Belts and Inner Magnetosphere, Geo- phys. Monogr. Ser., vol. 199, edited by D. Summers, I. R. Mann, D. N. Baker, and M. Schulz, pp. 255–264, American Geophysical Union, Washington, D. C., doi: 10.1029/2012GM001324.

Artemyev, A., Agapitov, O., Mourenas, D., Krasnoselskikh, V., Shastun, V., and Mozer, F. (2016), Oblique whistler- mode waves in the Earth's inner magnetosphere: Energy distribution, origins, and role in radiation belt dynamics, Space Sci. Rev., 200(1), 261– 355, doi:10.1007/s11214-016-0252-5.

Bell, T. F. (1984), The nonlinear gyroresonance interaction between energetic electrons and coherent VLF waves propagating at an arbitrary angle with respect to the Earth's magnetic field, J. Geophys. Res., 89(A2), 905–918.

Bortnik, J., R. M. Thorne, and U. S. Inan (2008a), Nonlinear interaction of energetic electrons with large amplitude chorus, Geophys. Res. Lett., 35, L21,102, doi:10.1029/ 2008GL035500.

Bortnik, J., R. M. Thorne, and N. P. Meredith (2008b), The unexpected origin of plasmaspheric hiss from discrete chorus emissions, Nature, 452, doi:10.1038/nature06741.

Burtis, W. J., and R. A. Helliwell (1975), Magnetospheric chorus: Amplitude and growth rate, J. Geophys. Res., 80(22), 3265–3270, doi:10.1029/JA080i022p03265.

Burton, R. K., and R. E. Holzer (1974), The origin and propagation of chorus in the outer magnetosphere, Journal of Geophysical Research, 79(7), 1014–1023, doi:10.1029/ JA079i007p01014.

Chen, L., W. Li, J. Bortnik, and R. M. Thorne (2012), Amplification of whistler-mode hiss inside the plasmasphere, Geophys. Res. Lett., 39, L08,111, doi:10.1029/2012GL051488.

Cornilleau-Wehrlin, N., J. Etcheto, and R. Burton (1976), Detailed analysis of magnetospheric ELF chorus: Preliminary results, Journal of Atmospheric and Terrestrial Physics, 38(11), 1201–1210, doi:10.1016/0021-9169(76)90052-0.

Gao, X., Li, W., Thorne, R. M., Bortnik, J., Angelopoulos, V., Lu, Q., Tao, X., and Wang, S. (2014), New evidence for generation mechanisms of discrete and hiss-like whistler mode waves, *Geophys. Res. Lett.*, 41, doi:10.1002/2014GL060707.

Gjerloev, J. W., Hoffman, R. A., Friel, M. M., Frank, L. A., and Sigwarth, J. B. (2004), Substorm behavior of the auroral electrojet indices, Ann. Geophys., 22, 2135– 2149, doi:10.5194/angeo-22-2135-2004.

Goldstein, J., B. R. Sandel, M. F. Thomsen, M. Spasojevic, and P. H. Reiff (2004), Simultaneous remote sensing and in situ observations of plasmaspheric drainage plumes, J. Geophys. Res., 109, A03202, doi:10.1029/2003JA010281.

Green, J. L., S. Boardsen, L. Garcia, W. Taylor, S. F. Fung, and B. Reinisch (2005), On the origin of whistler mode radiation in the plasmasphere, Journal of Geophysical Research: Space Physics, 110(A3), doi:10.1029/2004JA010495.

Hartley, D. P., Kletzing, C. A., Chen, L., Horne, R. B., & Santolík, O. (2019). Van Allen Probes observations of chorus wave vector orientations: Implications for the chorus-to-hiss mechanism. Geophysical Research Letters, 46, 2337–2346. https://doi.org/10.1029/2019GL082111

Helliwell, R. A. (1967), A theory of discrete VLF emissions from the magnetosphere, J. Geophys. Res., 72(19), 4773–4790.

Horne, R. B., S. A. Glauert, and R. M. Thorne (2003), Resonant diffusion of radiation belt electrons by whistler-mode chorus, Geophys. Res. Lett., 30(9), 1493, doi:10.1029/ 2003GL016963.

Horne, R. B., R. M. Thorne, Y. Y. Shprits, N. P. Meredith, S. A. Glauert, A. J. Smith, S. G. Kanekal, D. N. Baker, M. J. Engebretson, J. L. Posch, M. Spasojevic, U. S. Inan, J. S. Pickett, and P. M. E. Decreau (2005), Wave acceleration of electrons in the Van Allen radiation belts, Nature, 437, 227–230, doi:10.1038/nature03939.

Inan, U. S., T. F. Bell, and R. A. Helliwell (1978), Nonlinear pitch angle scattering of energetic electrons by coherent VLF waves in the magnetosphere, J. Geophys. Res., 83(A7), 3235–3253.

Kellogg, P. J., C. A. Cattell, K. Goetz, S. J. Monson, and L. B. Wilson III (2010), Electron trapping and charge transport by large amplitude whistlers, Geophys. Res. Lett., 37, L20,106, doi:10.1029/2010GL044845.

Kessel, R., N. Fox, and M. Weiss (2013), The radiation belt storm probes (RBSP) and space weather, Space Science Reviews, 179(1-4), 531–543, doi:10.1007/ s11214-012-9953-6.

Kletzing, C., W. Kurth, M. Acuna, R. MacDowall, R. Torbert, T. Averkamp, D. Bodet, S. Bounds, M. Chutter, J. Connerney, et al. (2013), The electric and magnetic field instrument suite and integrated science (EMFISIS) on RBSP, in The Van Allen Probes Mission, pp. 127–181, Springer, doi:10.1007/s11214-013-9993-6.

Kurth, W. S., S. De Pascuale, J. B. Faden, C. A. Kletzing, G. B. Hospodarsky, S. Thaller, and J. R. Wygant (2015), Electron densities inferred from plasma wave spectra obtained by the waves instrument on Van Allen Probes, J. Geophys. Res. Space Physics, 120(2), 904–914, doi:10.1002/2014JA020857.

Laakso, H., O. Santolik, R. Horne, I. Kolmasová, P. Escoubet, A. Masson, and M. Taylor (42), Identifying the source region of plasmaspheric hiss, Geophys. Res. Lett., pp. 3141– 3149, doi:10.1002/2015GL063755.

LeDocq, M. J., D. A. Gurnett, and G. B. Hospodarsky (1998), Chorus source locations from VLF Poynting flux measurements with the Polar spacecraft, Geophys. Res. Lett., 25(21), 4063–4066, doi:10.1029/1998GL900071.

Li, W., R. M. Thorne, V. Angelopoulos, J. Bortnik, C. M. Cully, B. Ni, O. LeContel, A. Roux, U. Auster, and W. Magnes (2009), Global distribution of whistler-mode chorus waves observed on the THEMIS spacecraft, Geophys. Res. Lett., 36, L09,104, doi: 10.1029/2009GL037595.

Li, W., J. Bortnik, R. M. Thorne, and V. Angelopoulos (2011a), Global distribution of wave amplitudes and wave normal angles of chorus waves using THEMIS wave observations, Geophys. Res. Lett., 116, A12,205, doi:10.1029/2011JA017035.

Li, W., R. M. Thorne, J. Bortnik, Y. Y. Shprits, Y. Nishimura, V. Angelopoulos, C. Chaston, O. L. Contel, and J. W. Bonnell (2011b), Typical properties of rising and falling tone chorus waves, Geophys. Res. Lett., 38, L14,103, doi:10.1029/2011GL047925.

Li, W., R. M. Thorne, J. Bortnik, X. Tao, and V. Angelopoulos (2012), Characteristics of hiss-like and discrete whistler-mode emissions, Geophys. Res. Lett., 39, L18,106, doi: 10.1029/2012GL053206.

Li, W., et al. (2013), An unusual enhancement of low-frequency plasmaspheric hiss in the outer plasmasphere associated with substorm-injected electrons, *Geophys. Res. Lett.*, 40, 3798– 3803, doi:10.1002/grl.50787.

Li, W., Q. Ma, R. M. Thorne, J. Bortnik, C. A. Kletzing, W. S. Kurth, G. B. Hospodarsky, and Y. Nishimura (2015), Statistical properties of plasmaspheric hiss derived from Van Allen Probes data and their effects on radiation belt electron dynamics. J. Geophys. Res. Space Physics, 120, 3393–3405. doi: 10.1002/2015JA021048.

Li, W., O. Santolik, J. Bortnik, R. Thorne, C. Kletzing, W. Kurth, and G. Hospodarsky (2016), New chorus wave properties near the equator from van allen probes wave observations, Geophysical Research Letters, 43(10), 4725–4735, doi:10.1002/2016GL068780.

Li, W., Shen, X.-C., Ma, Q., Capannolo, L., Shi, R., Redmon, R. J., et al (2019). Quantification of Energetic Electron Precipitation Driven by Plume Whistler Mode Waves, Plasmaspheric Hiss, and Exohiss. Geophysical Research Letters, 46. doi.org/10.1029/2019GL082095

Mauk, B., N. J. Fox, S. Kanekal, R. Kessel, D. Sibeck, and A. Ukhorskiy (2013), Science objectives and rationale for the radiation belt storm probes mission, Space Science Reviews, 179(1-4), 3–27, doi:10.1007/s11214-012-9908-y.

Meredith, N. P., A. D. Johnstone, S. Szita, R. B. Horne, and R. R. Anderson (1999), "Pancake" electron distributions in the outer radiation belts, J. Geophys. Res., 104(A6), 12,431–12,444, doi:10.1029/1998JA900083.

Meredith, N. P., R. B. Horne, R. M. Thorne, and R. R. Anderson (2003), Favored regions for chorus-driven electron acceleration to relativistic energies in the Earth's outer radiation belt, Geophys. Res. Lett., 30(16,1871), doi:10.1029/2003GL017698.

Meredith, N. P., Horne, R. B., Thorne, R. M., Summers, D., and Anderson, R. R. (2004), Substorm dependence of plasmaspheric hiss, *J. Geophys. Res.*, 109, A06209, doi:10.1029/2004JA010387.

Meredith, N. P., R. B. Horne, A. Sicard-Piet, D. Boscher, K. H. Yearby, W. Li, and R. M. Thorne (2012), Global model of lower band and upper band chorus from multiple satellite observations, J. Geophys. Res., 117, A10,225, doi:10.1029/2012JA017978.

Meredith, N. P., R. B. Horne, J. Bortnik, R. M. Thorne, L. Chen, W. Li, and A. Sicard-Piet (2013), Global statistical evidence for chorus as the embryonic source of plasmaspheric hiss, Geophys. Res. Lett., 40, 2891–2896, doi:10.1002/grl.50593.

Meredith, N. P., Horne, R. B., Kersten, T., Li, W., Bortnik, J., Sicard, A., & Yearby, K. H. (2018). Global model of plasmaspheric hiss from multiple satellite observations. *Journal of Geophysical Research: Space Physics*, 123, 4526– 4541. https://doi.org/10.1029/2018JA025226

Moldwin, M. B., L. Downward, H. Rassoul, R. Amin, and R. Anderson (2002), A new model of the location of the plasmapause: Crres results, Journal of Geophysical Research: Space Physics, 107(A11), SMP–2, doi:10.1029/2001JA009211.

Nakamura, S., Omura, Y., & Summers, D. (2018). Fine structure of whistler mode hiss in plasmaspheric plumes observed by the Van Allen Probes. *Journal of Geophysical Research: Space Physics*, 123, 9055– 9064. https://doi.org/10.1029/2018JA025803

Ni, B., R. M. Thorne, Y. Y. Shprits, and J. Bortnik (2008), Resonant scattering of plasma sheet electrons by whistler-mode chorus: Contribution to diffuse auroral precipitation, Geophys. Res. Lett., 35, L11106, doi:10.1029/2008GL034032.

Ni, B., R. M. Thorne, X. Zhang, J. Bortnik, Z. Pu, L. Xie, Z.-J. Hu, D. Han, R. Shi, C. Zhou, and X. Gu (2016), Origins of the Earth's diffuse auroral precipitation, Space Sci. Rev., 200(1), 205-259, doi:10.1007/s11214-016-0234-7.

Nishimura, Y., J. Bortnik, W. Li, R. M. Thorne, L. R. Lyons, V. Angelopoulos, S. B. Mende, J. W. Bonnell, O. L. Contel, C. Cully, R. Ergun, and U. Auster (2010), Identifying the driver of pulsating aurora, Science, 330(6000), 81–84, doi:10.1126/science. 1193130.

Nunn, D. (1971), A theory of VLF emissions, Planet. Space Sci., 19, 1141–1167. Omura, Y., N. Furuya, and D. Summers (2007), Relativistic turning acceleration of resonant electrons by coherent whistler mode waves in a dipole magnetic field, J. Geophys. Res., 112, A06,236, doi:10.1029/2006JA012243.

Omura, Y., Y. Katoh, and D. Summers (2008), Theory and simulation of the generation of whistler-mode chorus, J. Geophys. Res., 113, A04,223, doi:10.1029/2007JA012622.

Reeves, G. D., H. E. Spence, M. G. Henderson, S. K. Morley, R. H. W. Friedel, H. O. Funsten, D. N. Baker, S. G. Kanekal, J. B. Blake, J. F. Fennell, S. G. Claudepierre, R. M. Thorne, D. L. Turner, C. A. Kletzing, W. S. Kurth, B. A. Larsen, and J. T. Niehof (2013), Electron acceleration in the heart of the Van Allen radiation belts, Science, 341(6149), 991–994, doi:10.1126/science.1237743.

Funsten, D. N. Baker, S. G. Kanekal, J. B. Blake, J. F. Fennell, S. G. Claudepierre, R. M. Thorne, D. L. Turner, C. A. Kletzing, W. S. Kurth, B. A. Larsen, and J. T. Niehof (2013), Electron acceleration in the heart of the Van Allen radiation belts, Science, 341(6149), 991–994, doi:10.1126/science.1237743.

Santolík, O., D. A. Gurnett, J. S. Pickett, M. Parrot, and N. Cornilleau-Wehrlin (2003), Spatio-temporal structure of storm-time chorus, J. Geophys. Res., 108(A7), 1278, doi: 10.1029/2002JA009791.

Santolík, O., D. A. Gurnett, J. S. Pickett, M. Parrot, and N. Cornilleau-Wehrlin (2004), A microscopic and nanoscopic view of storm-time chorus on 31 March 2001, Geophys. Res. Lett., 31, L02,801, doi:10.1029/2003GL018757.

Santolík, O., Gurnett, D. A., Pickett, J. S., Chum, J., and Cornilleau-Wehrlin, N. (2009), Oblique propagation of whistler mode waves in the chorus source region, *J. Geophys. Res.*, 114, A00F03, doi:10.1029/2009JA014586.

Shi, R., W. Li, Q. Ma, A. Green, C. A. Kletzing, W. S. Kurth, G. B. Hospodarsky, S. G. Claudepierre, H. E. Spence, and G. D. Reeves (2019), Properties of whistler mode waves in earth's plasmasphere and plumes, Journal of Geophysical Research: Space Physics, doi:10.1029/2018JA026041.

Solomon, J., Cornilleau-Wehrlin, N., Korth, A., and Kremser, G. (1988), An experimental study of ELF/VLF hiss generation in the Earth's magnetosphere, *J. Geophys. Res.*, **93**, 1839.

Soto-Chavez, A. R., G. Wang, A. Bhattacharjee, G. Y. Fu, and H. M. Smith (2014), A model for falling-tone chorus, Geophys. Res. Lett., 41, 1838–1845, doi:10.1002/ 2014GL059320.

Su, Z., N. Liu, H. Zheng, Y. Wang, and S. Wang (2018), Large-amplitude extremely low frequency hiss waves in plasmaspheric plumes, Geophysical Research Letters, 45(2), 565–577, doi:10.1002/2017GL076754.

Summers, D., B. Ni, N. P. Meredith, R. B. Horne, R. M. Thorne, M. B. Moldwin, and R. R. Anderson (2008), Electron scattering by whistler-mode ELF hiss in plasmaspheric plumes, J. Geophys. Res., 113, A04,219, doi:10.1029/2007JA012678.

Tao, X., and J. Bortnik (2010), Nonlinear interactions between relativistic radiation belt electrons and oblique whistler mode waves, Nonlin. Processes Geophys., 17, 599–604, doi:10.5194/npg-17-599-2010.

Tao, X., R. M. Thorne, W. Li, B. Ni, N. P. Meredith, and R. B. Horne (2011), Evolution of electron pitch angle distributions following injection from the plasma sheet, J. Geo- phys. Res., 116, A04,229, doi:10.1029/2010JA016245.

Tao, X., J. Bortnik, R. M. Thorne, J. Albert, and W. Li (2012), Effects of amplitude modulation on nonlinear interactions between electrons and chorus waves, Geophys. Res. Lett., 39, L06,102, doi:10.1029/2012GL051202.

Tao, X., F. Zonca, and L. Chen (2017a), Identify the nonlinear wave-particle interaction regime in rising tone chorus generation, Geophys. Res. Lett., 44(8), 3441–3446, doi: 10.1002/2017GL072624, 2017GL072624.

Tao, X., F. Zonca, and L. Chen (2017b), Investigations of the electron phase space dynamics in triggered whistler wave emissions using low noise δ f method, Plasma Phys. Controlled Fusion, 59(9), 094,001, doi:10.1088/1361-6587/aa759a.

Taubenschuss, U., Y. V. Khotyaintsev, O. Santolík, A. Vaivads, C. M. Cully, O. L. Contel, and V. Angelopoulos (2014), Wave normal angles of whistler mode chorus rising and falling tones, J. Geophys. Res. Space Physics, 119(12), 9567–9578, doi:10.1002/ 2014JA020575.

Taubenschuss, U., O. Santolík, D. B. Graham, H. Fu, Y. V. Khotyaintsev, and O. L. Contel (2015), Different types of whistler mode chorus in the equatorial source region, Geo- phys. Res. Lett., 42(20), 8271–8279, doi:10.1002/2015GL066004.

Thorne, R. M., E. J. Smith, R. K. Burton, and R. E. Holzer (1973), Plasmaspheric hiss, J. Geophys. Res., 78(10), 1581–1596.

Thorne, R. M., B. Ni, X. Tao, R. B. Horne, and N. P. Meredith (2010), Scattering by chorus waves as the dominant cause of diffuse auroral precipitation, Nature, 467, 943–946, doi:10.1038/nature09467.

Thorne, R. M., W. Li, B. Ni, Q. Ma, J. Bortnik, L. Chen, D. N. Baker, H. E. Spence, G. D. Reeves, M. G. Henderson, C. A. Kletzing, W. S. Kurth, G. B. Hospodarsky, J. B. Blake, J. F. Fennell, S. G. Claudepierre, and S. G. Kanekal (2013), Rapid local acceleration of relativistic radiation belt electrons by magnetospheric chorus, Nature, 504, 411–414, doi:10.1038/nature12889.

Trakhtengerts, V. Y. (1995), Magnetosphere cyclotron maser: Backward wave oscillator generation regime, J. Geophys. Res., 100(A9), 17,205–17,210.

Tsurutani, B. T., and E. J. Smith (1974), Postmidnight chorus: A substorm phenomenon, J. Geophys. Res., 79(1), 118–127.

Tsurutani, B. T., and E. J. Smith (1977), Two types of magnetospheric ELF chorus and their substorm dependences, J. Geophys. Res., 82(32), 5112–5128, doi:10.1029/ JA082i032p05112.

Tsurutani, B. T., B. J. Falkowski, J. S. Pickett, O. Santolik, and G. S. Lakhina (2015), Plasmaspheric hiss properties: Observations from Polar, Journal of Geophysical Research: Space Physics, 120(1), 414–431, doi:10.1002/2014JA020518.

Tsyganenko, N., and M. Sitnov (2005), Modeling the dynamics of the inner magnetosphere during strong geomagnetic storms, J. Geophys. Res, 110, A03208, doi:10.1029/ 2004JA010798.

Vomvoridis, J. L., T. L. Crystal, and J. Denavit (1982), Theory and computer simulations of magnetospheric very low frequency emissions, J. Geophys. Res., 87(A3), 1473–1489, doi:10.1029/JA087iA03p01473.

Wygant, J., J. Bonnell, K. Goetz, R. Ergun, F. Mozer, S. Bale, M. Ludlam, P. Turin, P. Harvey, R. Hochmann, et al. (2013), The electric field and waves instruments on the radiation belt storm probes mission, Space Science Reviews, 179(1-4), 183–220, doi: 10.1007/s11214-013-0013-7.

Zhang, W., S. Fu, X. Gu, B. Ni, Z. Xiang, D. Summers, Z. Zou, X. Cao, Y. Lou, and M. Hua (2018), Electron scattering by plasmaspheric hiss in a nightside plume, Geophys. Res. Lett., 45, 4618-4627, doi:10.1029/2018GL077212.

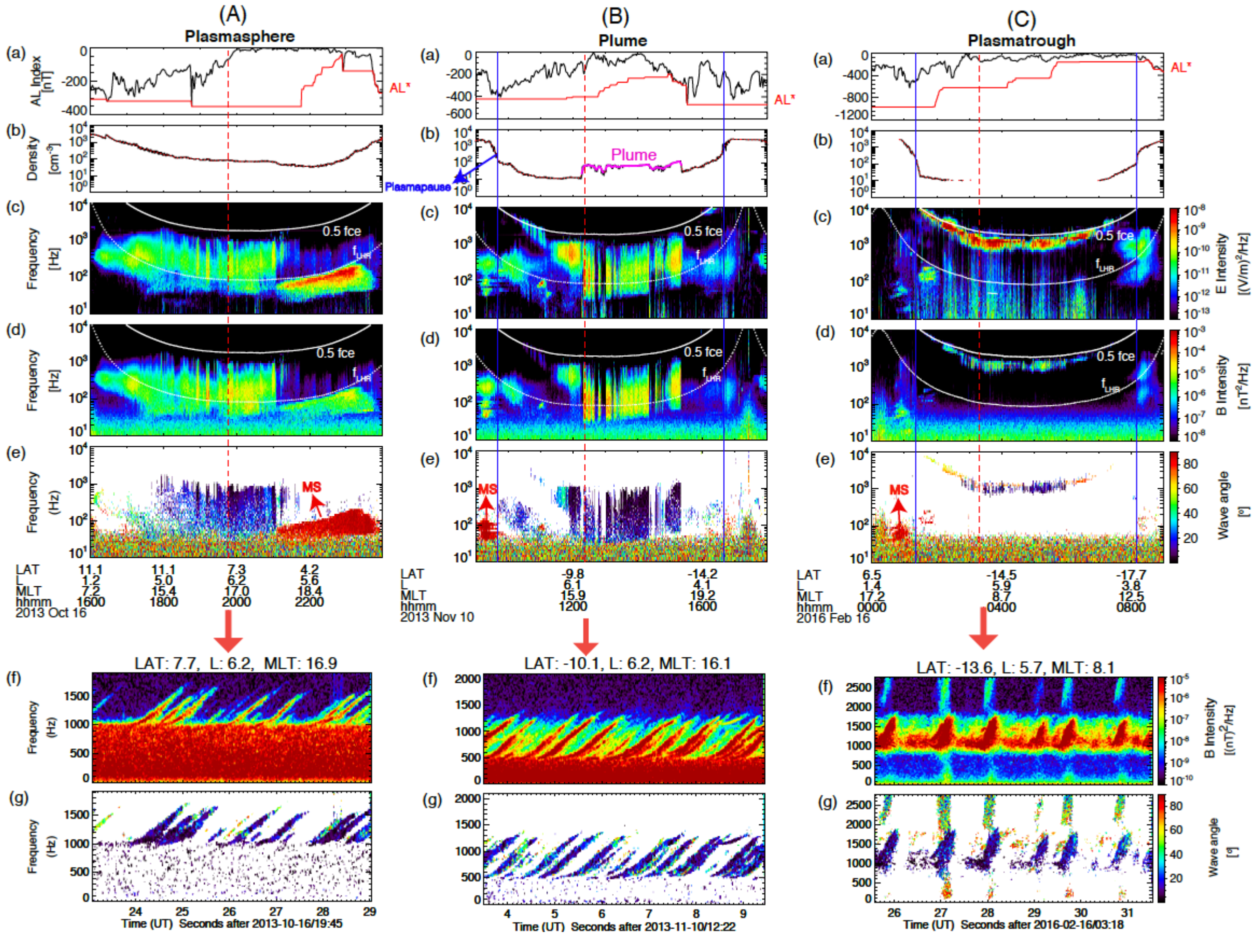

Figure 1. Three examples of rising tone whistler mode waves observed (A) inside the plasmasphere, (B) plasmaspheric plume, and (C) plasmatrough. (a) AL (black) and AL* (red). (b) Plasma density inferred from the upper hybrid resonance line, where the magenta line corresponds to the density in plume regions. (c) Electric spectral density, (d) magnetic spectral density, and (e) wave normal angle. In Figures 1c and 1d, the white lines represent 0.5 f_{ce} (dashed) and f_{LHR} (dotted), where f_{ce} and f_{LHR} are electron cyclotron frequency and lower hybrid resonance (LHR) frequency respectively. The vertical blue lines indicate the plasmapause crossing. The vertical red dashed lines denote the three occasions when the burst mode data were captured. The bottom panels show (f) the magnetic wave spectra and (g) wave normal angle using burst mode data.

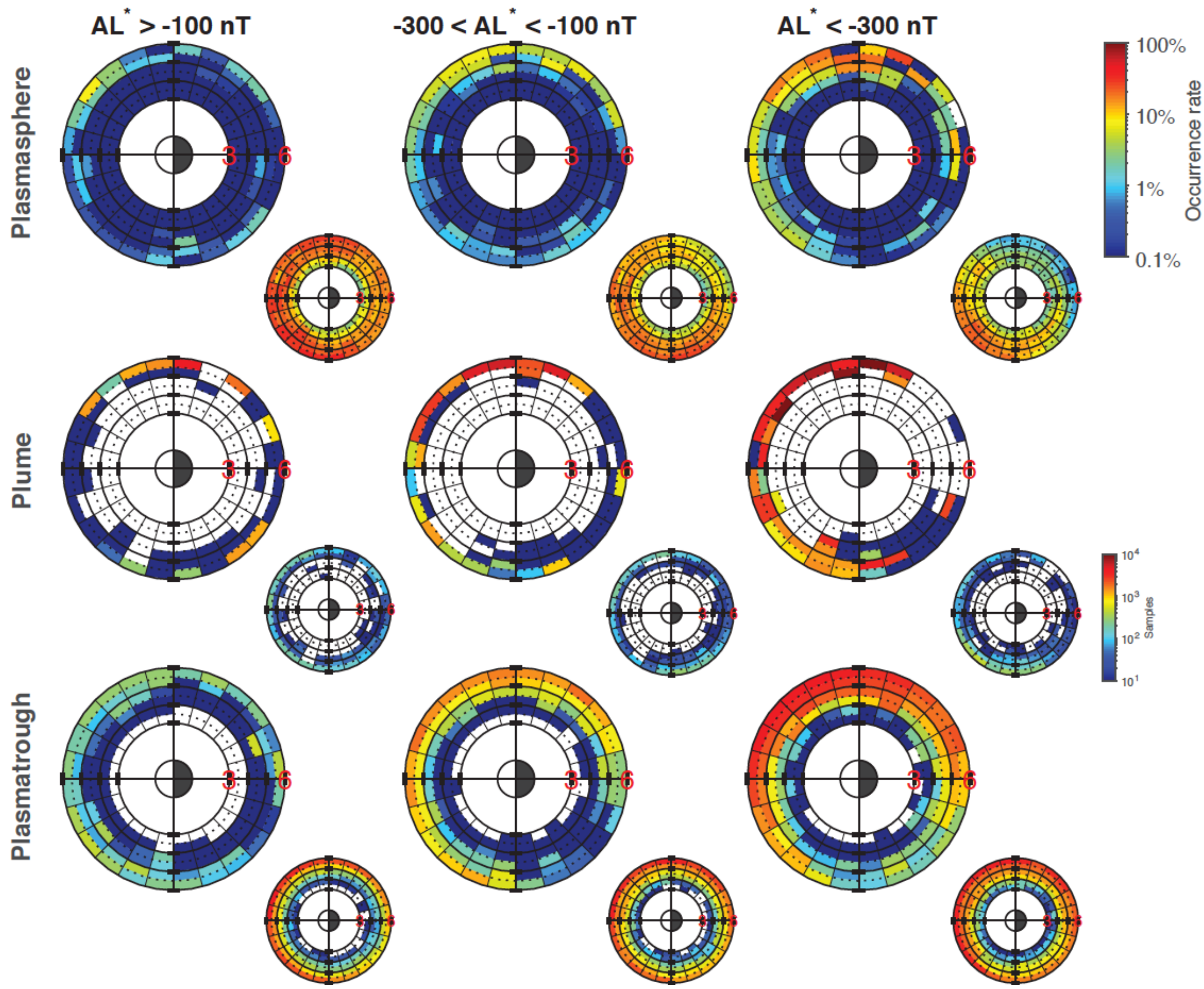

Figure 2. The L-MLT distribution of the occurrence rate of rising tone whistler mode waves observed inside the plasmasphere (top), plasmaspheric plumes (middle), and plasmatrough (bottom) for different levels of AL*. The corresponding distribution of number of samples is shown in the small panels. The bin size is 1 hour in MLT and 0.5 in *L*.

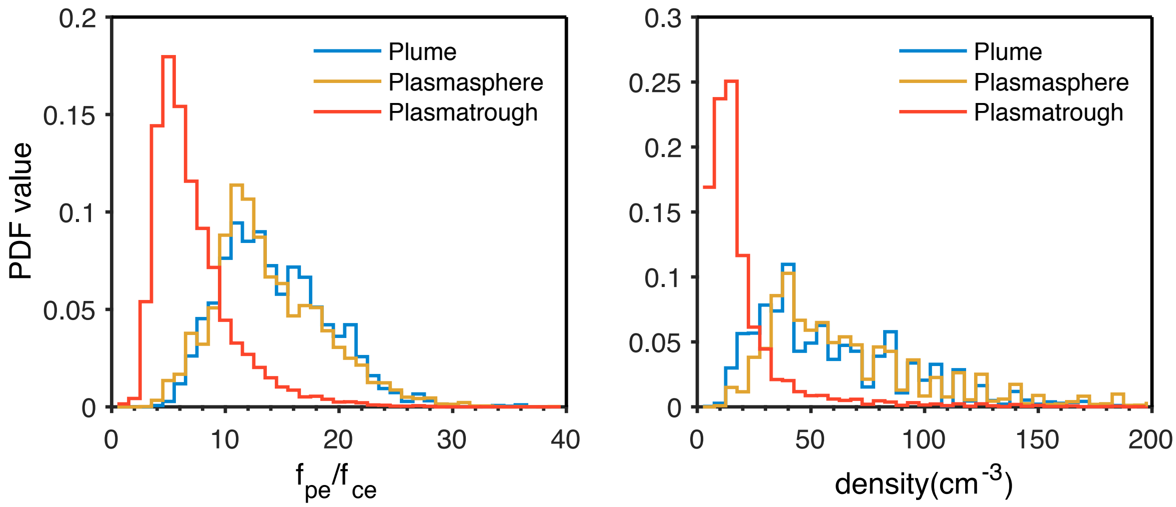

Figure 3. The probability distribution function of density and the ratio of plasma frequency (f_{pe}) to electron cyclotron frequency (f_{ce}) for rising tone whistler mode wave events in three different regions: inside the plasmasphere (yellow), plasmaspheric plumes (blue) and plasmatrough (red).

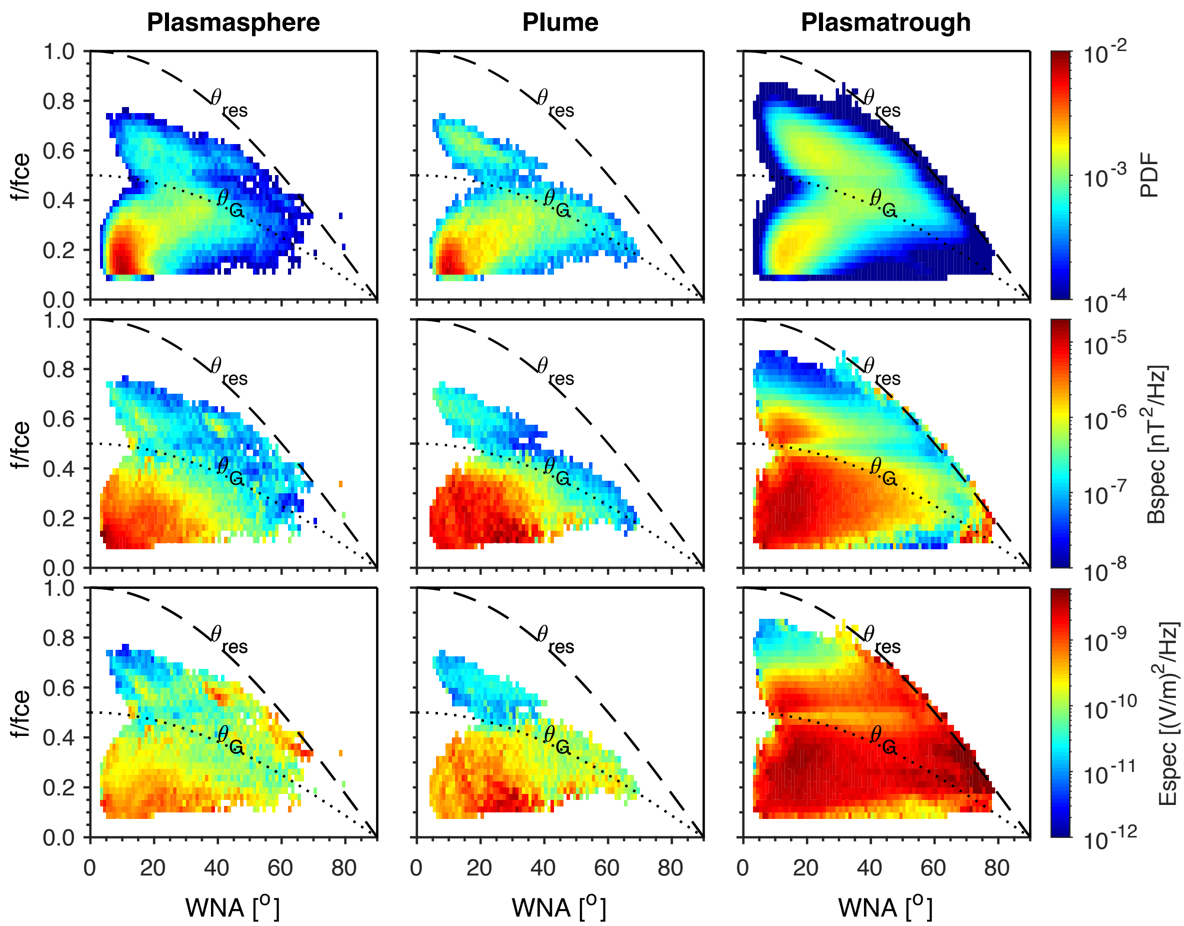

Figure 4. The normalized frequency and wave normal angle distribution of rising tone whistler mode waves in three different regions: inside the plasmasphere (left column), in plasmaspheric plumes (middle column), and plasmatrough (right column). The top to bottom rows are the probability distribution function (PDF) of wave occurrences (top), the average magnetic (middle) and electric power spectral density (bottom). The dashed lines indicate the resonance cone angle estimated using arccos(f/f_{ce}), and the dotted lines indicate the Gendrin angle calculated using arccos($2f/f_{ce}$).